Indian Journal of Pure & Applied Physics
Vol. 55, February 2017, pp. 129-134

Current conduction in Schottky barrier diodes with poly(propylene glycol)-b-polystyrene block copolymer interfacial layer

Mert Yildirim[a]*, Abdulkadir Alli[b], Ahmet Demir[c], Sema Alli[d] & Muharrem Gokcen[c]

[a]Department of Mechatronics Engineering, Faculty of Engineering, Düzce University, Konuralp, 81620, Turkey
[b]Department of Chemistry, Faculty of Arts & Sciences , Düzce University, Konuralp, 81620, Turkey
[c]Department of Physics, Faculty of Arts & Sciences, Düzce University, Konuralp, 81620, Turkey
[d]Department of Polymer Engineering, Faculty of Technology, Düzce University, Konuralp, 81620, Turkey

Received 16 February 2016; revised 2 September 2016; accepted 26 December 2016

Polymeric materials have gained great importance in electron devices. There has been considerable number of studies on block copolymers due to enhanced features that appear after co-polymerization. In this study, poly (propylene glycol)-b-polystyrene block copolymer has been synthesized and Schottky barrier diodes (SBDs) have been fabricated with this block copolymer. Current-voltage (*I-V*) measurements have been conducted at room temperature in order to investigate electrical characteristics and current conductions governing in these SBDs. Series resistance and shunt resistance of the SBDs have been calculated using Ohm's law. Ideality factor, reverse saturation current and zero-bias barrier height of the SBDs have been extracted from the forward-bias *I-V* data. Fabricated SBDs exhibited high rectifying ratio of the order 10^4. Also, current conduction mechanisms and the density of interface states in the SBDs have been investigated. Calculated values of density of interface states in the SBDs are on the order of 10^{13} which is acceptable for this kind of SBDs having polymeric interfacial layer.

Keywords: Polymer composites, Block copolymers, Electrostatic spraying, Polymeric nanofiber, Current conduction

1 Introduction

Polymeric materials are used in many optoelectronic applications since these materials can be prepared in the form of film by easy processing techniques such as electrostatic spraying, spin coating, dip coating, sol–gel, solution casting etc[1-14]. Also, one of the advantages of polymeric materials is that physical, chemical and electrical properties of these polymeric materials can be controlled by addition of some reagents into the polymer solution. Besides conventional coating methods, polymers can be coated on surfaces through electrostatic spraying. This method allows formation of polymeric nanofibers and these fibers can enhance the efficiency due to increasing electrical and optical interaction with the nanofiber surface. For this reason, there are many studies in the literature which cover investigation of commercial polymers[3-16]. Nevertheless, electro-optical properties of synthesized polymers and possible applications of them in device technologies have become an attractive investigation area for the researchers.

Block copolymers have been used in various applications of humidity sensor, biomedical, plastic research, hydrophobic/hydrophilic surface, injectable drug-delivery systems, optoelectronics and Schottky barrier diodes[16-23]. Especially, polystyrene-b-poly(ethylene glycol) (PS-b-PPEG) and polystyrene-b-poly (propylene glycol) (PS-b-PPG) block copolymers were studied by various researchers in the last decade[22-25]. These polymers can be prepared by various types of macro initiators through radical and ionic polymerization. Macro initiators generating radicals can be classified as macro-azo-initiators, azo peroxidic initiators, redox macroinitiators[26,27] and macrophotoinitiators[28]. Macro-azo-initiators which can be prepared by the condensation reactions of a prepolymer with azobis-isobutyronitrile[29-33], 4, 4_azobis (4-cyanopentanoyl chloride)[34], 4,4_azobiscyanopentanol[35], provide useful means of preparing amphiphilic block copolymers via radical process.

In our previous studies, we investigated electrical parameters of metal-polymer-semiconductor (MPS) structure having poly (propylene glycol)-b-polystyrene (PPG-b-PS) block copolymer layer under UV and visible illumination[36,37]. PPG-b-PS block copolymer proved itself suitable for MPS structures, in this study we prepared SBDs with PPG-b-PS and with PPG-b-PS dispersed with $HAuCl_4$. Since PPG-b-PS was found promising material for MPS structures, we also aimed to investigate possible current conduction mechanisms in

*Corresponding author (E-mail: mertyildirim@duzce.edu.tr)

SBDs having PPG-b-PS interfacial layer. Therefore, we fabricated Au/PPG-b-PS/n-Si (MPS1) and Au/PPG-b-PS ($HAuCl_4$ dispersed)/n-Si (MPS2) SBDs. Besides its utility in biomedical and plastic research areas, this study aims to explore further the utility of PPG-b-PS in SBDs in terms of current conduction mechanisms.

2 Experimental Details

For the synthesis of block copolymer, PPG-b-PS, 4,4′-Azobis-4-cyanopentanoic acid (ACPA) was purchased from Fluka AG, poly (propylene) bis (2-aminopropyl ether) (PPG-NH_2) (amine groups at both ends of each chain) of average MW 400 and MW 2000 was purchased from Aldrich and Styrene was purchased from Merck. Moreover, utilized solvents and other reagents were chosen among extra pure commercial products for reliable results. Styrene was dried with Na_2SO_4 and freshly distilled under reduced pressure before use. 4,4′-azobis-4-cyanopentanoyl chloride (ACPC) was prepared by the reaction of ACPA with phosphorus penta chloride which was carried out in benzene at room temperature. For the synthesis of macro azo initiator, a solution of 2.0 g (6.3 mmol) of ACPC in 50 mL $CHCl_3$ was added to the mixture of 25.24 g (12.6 mmol) of poly(propylene) bis (2-aminopropyl ether) (PPG-NH_2-2000) and 10 mL of aqueous NaOH (20 wt%) and stirred for 24 h at room temperature. The molar ratio of ACPC to PPG-2000 was 1:2. After the reaction, the mixture was washed with water three times to ensure the removal of salts and ACPA from the product. The organic phase was dried with Na_2SO_4 overnight at 0 °C. Later, solvent was evaporated and viscous liquid was dried under vacuum and stored at 0 °C until use. For the synthesis of PPG-b-PS block copolymer, a given amount of styrene and the macro initiator (MI-PPG) were charged into a Pyrex tube. Nitrogen was introduced through a needle into the tube to expel the air. The tightly capped tube containing a small magnet was put in an oil bath at 80 °C for 5 h. Subsequently the contents of the tube were dissolved in chloroform and then precipitated in methanol. The co polymeric sample obtained was dried in vacuum at room temperature for 24 h. For the fabrication of SBDs, n-type (P-doped) single crystal silicon wafer with <100> surface orientation, 500 μm thickness, with 2" diameter and 1-10 Ω.cm resistivity was chosen as semiconductor material. Following the chemical cleaning process, details[35,36], back surface of the n-Si was deposited with high purity Ag metal (99.999 %) 250 nm thick from the tungsten filament in vacuum environment of 1×10^{-6} Torr. For obtaining good ohmic behavior, the evaporated Ag was annealed at 500 °C for 30 min. Later, front side of the wafer was cleaned with 20% HF solution to remove the thin oxide layer formed during annealing. Then, the wafer was cut into 2 pieces. For the electrostatic spraying process, poly (propylene glycol)-b-polystyrene block copolymer was prepared as 5% in N,N-Dimethylformamide (DMF) solution in two tubes and later a drop of $HAuCl_4$ as % 0.2 in DMF solution was dispersed in one of the tubes. After, prepared polymeric solutions were sprayed onto the front side of the Si wafer pieces through an electrostatic spraying (Inovenso, Turkey) system. The solutions for spraying was loaded into a 10 mL hypodermic stainless steel syringe with a nozzle (0.8 mm in diameter) connected to a digitally-controlled pump which provides a constant flow rate of 0.8 mL/h. The Si wafer was placed on the collector distance from the metal nozzle was kept at 15 cm. Upon applying a high voltage of 28 kV to the nozzle, a fluid jet was ejected from the nozzle. Later, using a metal mask, polymeric face of the substrate was deposited with high purity Au metal (99.999%) having thickness of 250 nm from the tungsten filament in vacuum environment of 1×10^{-6} Torr. Schematic diagram of the fabricated SBDs with chemical structure of PPG-b-PS block copolymer is shown in Fig. 1.

For the morphology of polymeric films, a FEI QUANTA FEG Scanning Electron Microscope (SEM) is used. Current-voltage (*I-V*) measurements of the SBDs were held by a Keithley 2400 source-meter at room temperature.

3 Results and Discussion

3.1 Analysis of SEM micrographs

SEM micrographs of the polymer interfacial surfaces are presented in Fig. 2(a) and (b). The average fiber diameter for PPG-b-PS nanofibers is about 300 nm. As seen in Fig. 2(b), average fiber diameter is about same suggesting that $HAuCl_4$ dispersal does not create a prominent effect on fiber size. Regarding other SEM results of various polymers in other studies utilizing electrostatic

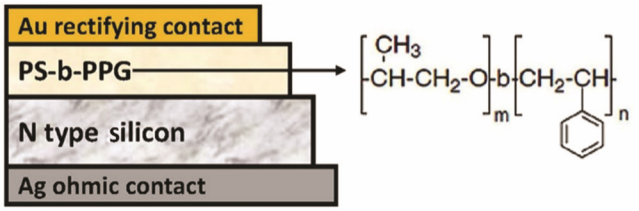

Fig. 1 — Schematic diagram of the SBDs with chemical structure of poly (propylene glycol)-b-polystyrene

spraying[3-8], we can reach the conclusion that electrostatic spraying method is successful in fabricating polymeric nanofibers from PPG-b-PS because nanofiber formation is almost homogeneous for both SBDs.

3.2 Analysis of current-voltage (*I-V*) characteristics

I-V plots of the SBDs are given in Fig. 3. The inset of Fig. 3 provides the same data in the form of semi-logarithmic forward and reverse *I-V* plots. Thus, it is possible to deduce a general idea about the various electrical parameters of the SBDs. At first look, it is obvious that both SBDs exhibit typical feature of a SBD; leakage current at very low levels and sudden increase in current in the forward bias region. Considering the *I-V* data in forward bias region, current increases almost linearly for MPS1 (see inset of Fig. 3) indicating ohmic conduction must be dominant in this region. Also MPS2, *I-V* curve bends in this region therefore MPS2 likely has higher R_s considering what was reported about these kind of structures in literature.[1,11-13,38]

As can be seen in the semi-logarithmic plots, MPS1 has lower leakage current values whereas it has higher current values in the forward bias region, hence it has higher rectifying ratio (RR). Calculated RR values for MPS1 and MPS2 are 7.1×10^4 and 2.6×10^4, respectively. MPS1 structure shows better rectifying feature depending on the SBD's resistivity in the high forward and reverse bias regions. Therefore, it can be said that MPS1 and MPS2 exhibit fairly good rectifying feature compared with findings of other studies.[2,3,9,11-12,15,39]

There are various methods for obtaining a SBD's resistivity in the literature[40-42]. An easy and practical way of calculating shunt and series resistance is Ohm's law where resistance (R_i) value is given by R_i=dV/dI. Figure 4 shows semi-logarithmic R_i-V plots of the SBDs. It is well known that R_i corresponds to R_s at sufficiently high forward bias voltages and R_{sh} at sufficiently high reverse bias voltages. Therefore, it can be said that MPS2 has lower R_{sh} and higher R_s compared to MPS1. The resistance values are given in Table 1, along with the other calculated electrical parameters. As can be seen in Table 1, obtained R_s values can be regarded as low considering the R_s values of various commercial organic material based devices in the literature.[11-13,15,39]

Table 1 — Electrical parameters of the SBDs obtained from *I-V* plots

	R_{sh} (MΩ)	R_s (Ω)	I_o (pA)	n	Φ_{B0} (eV)
MPS1	72.5	258	174	2.53	0.93
MPS2	43.1	315	50	2.29	0.96

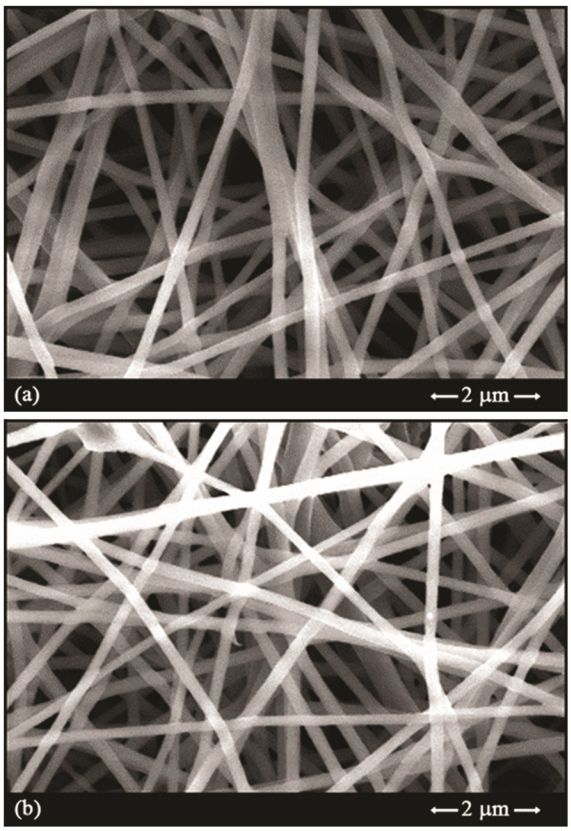

Fig. 2 — SEM micrographs of (a) PPG-b-PS and (b) PPG-b-PS + $HAuCl_4$ films

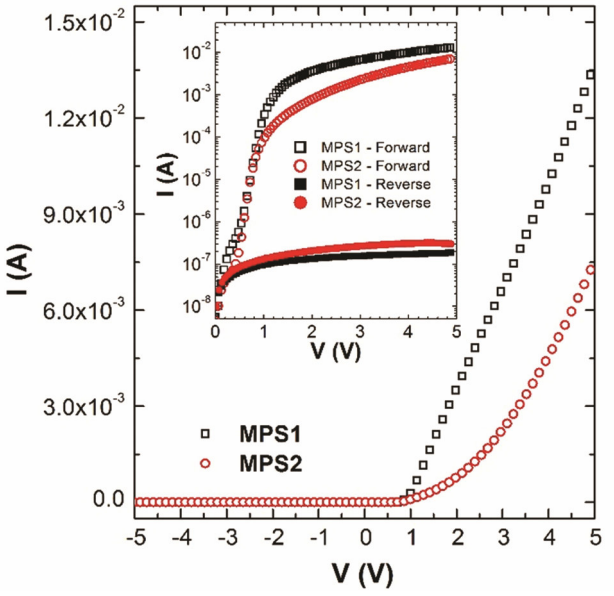

Fig. 3 — *I–V* plots of the SBDs at room temperature. Inset shows the semi-logarithmic *I–V* plots

In Fig. 3, semi-logarithmic *I-V* curves of both SBDs exhibit a linear region between 0.5 V and 1 V by which some of the main electrical parameters can be obtained. When electrical characteristics of a SBD is considered, the relationship between current and applied bias voltage can be given through following equation on the basis of thermionic emission (TE) theory where $V \geq 3kT/q$ holds[2,9,11,12,15,39,43-45]:

$$I = I_o \left[\exp\left(\frac{q(V - IR_s)}{nkT} \right) - 1 \right] \quad \ldots (1)$$

Here, n is ideality factor, T is absolute temperature in Kelvin, k is Boltzmann constant, q is the electronic charge, R_s is series resistance and I_o is reverse saturation current, respectively. Reverse saturation current is given by[2,9,11,12,15,39,43-45]:

$$I_o = AA^* T^2 \exp\left(-\frac{q\Phi_{B0}}{kT} \right) \quad \ldots (2)$$

where A^*, A and Φ_{B0} are effective Richardson constant (120 A/cm^{2}K^2 for n-Si), area of rectifying contact and zero-bias barrier height, respectively.

Using Eq. (1), the values of n and I_0 can be obtained from the slope and interception point of the line through the linear region between 0.5 V and 1 V. Once I_o is obtained, Φ_{B0} can easily be calculated using Eq. (2). I_o, n and Φ_{B0} values of the SBDs are given in Table 1. As can be seen, MPS1 has higher I_o and n values whereas it has lower Φ_{B0} value. Obtained n values are not very large, they can even be considered moderate for these SBDs with polymeric interfacial layer n values obtained for the studied SBDs are fair when compared with those obtained by various researchers in the literature[3,9,11-13,15,39,44,45].

It is reported that several type of current conduction mechanisms are governed in the forward bias region of these kind of SBDs[2,13]. In many studies, TE is used to extract the electrical parameters of the structure; however obtained results for these parameters may not be precise depending on how large the n value is. It is well known that n shows the conformity of *I-V* data to TE. Hence, it is an indication of deviation from TE to obtain n value larger than 1. For the purpose of investigating possible mechanisms, ln*I*-ln*V* plots of the SBDs are given in Fig. 5.

As can be seen in Fig. 5, ln*I*-ln*V* curves of both SBDs have three linear regions. The slope of these regions yields the m value in the proportionality of $I \alpha V^m$. In Region 1, m value of MPS1 is close to 2.This means that the dominant current conduction mechanism (CCM) in this region is space charge-limited current (SCLC)[13,46]. For the same region, m value of MPS2 is very close to 1, which means that CCM of the structure is almost ohmic conduction. In Region 2, m values of MPS1 and MPS2 are 10.8 and 10.2, respectively. It is known that the CCM is trap-filled SCLC when m value[13,46] is larger than 2. Therefore, in this region, current is transported by trap-filled SCLC. In Region 3, m value of MPS1 is 1.39. This indicates that the dominant CCM in this region is ohmic conduction for MPS1. This result is also consistent with linear increase in current with applied bias in the high forward bias region for MPS1 (see Fig. 3). On the other hand, m value of MPS2 in

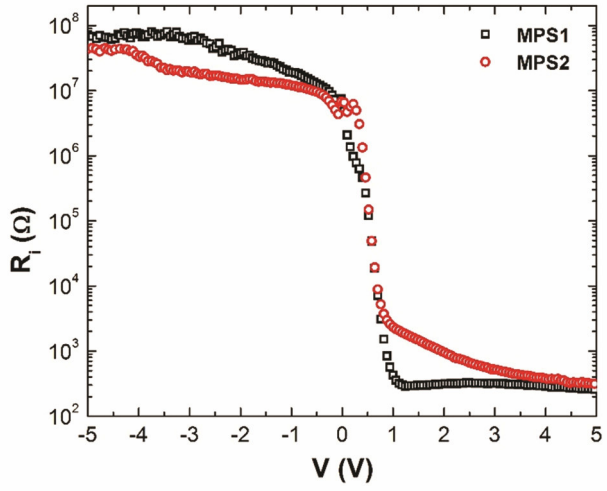

Fig. 4 — Semi-logarithmic R_i–V plots of the SBDs at room temperature

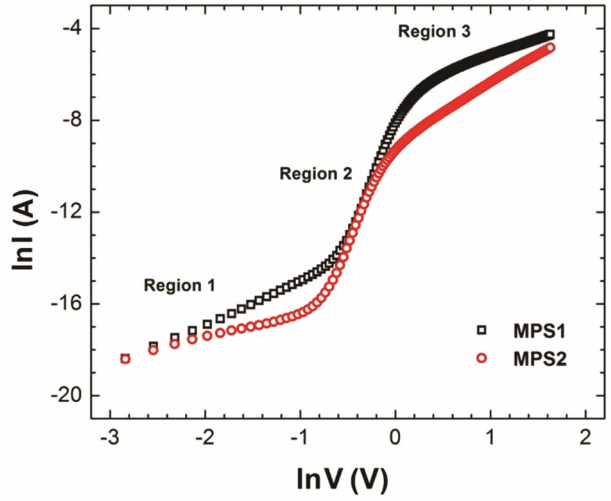

Fig. 5 — ln*I*–ln*V* plots of the SBDs at room temperature

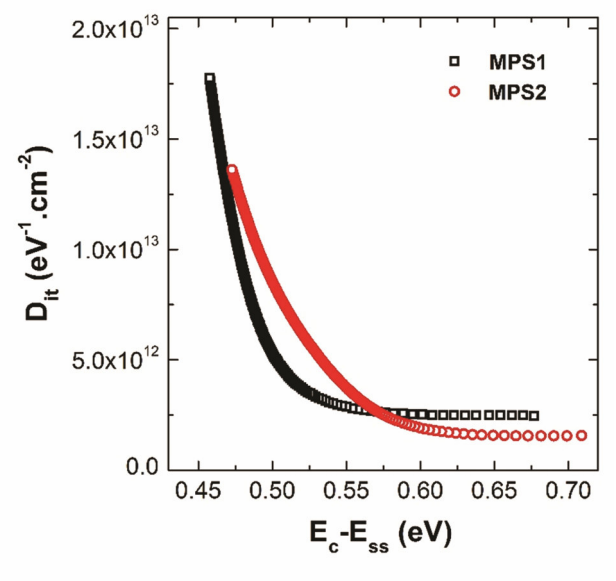

Fig. 6 — D_{it}–E_c-E_{ss} plots of the SBDs at room temperature

this region is 2.54, therefore it can be said that CCM in MPS2 deviates from SCLC to trap-filled SCLC.

Density of interface states (D_{it}) in the studied SBDs were calculated using card and Rhoderick's function[47] which gives voltage dependent ideality factor, $n(V)$, as a function of D_{it} as:

$$n(V) = 1 + \frac{d}{\varepsilon_i}\left(\frac{\varepsilon_s}{W_D} + qD_{it}(V)\right) \quad \ldots (3)$$

where d, ε_i, ε_s and W_D are thickness of polymeric layer, permittivity of polymeric layer, permittivity of semiconductor and depletion layer width. Calculated D_{it} values of the SBDs are presented in Fig. 6 as D_{it} – E_c-E_{ss} plots. Details of calculating E_c-E_{ss} values are given in elsewhere[1,11,12].

As can be seen in Fig. 6, D_{it} of both SBDs is on the order of 10^{13} $eV^{-1}.cm^{-2}$ this can be regarded moderate for couple reasons: (i) similar results were obtained for different types of SBDs with polymeric interfacial layer in the literature[11,12,15,39] and (ii) obtained D_{it} value for both SBDs is lower than that of a Au/n-Si SBD[44] . It is seen that D_{it} increases exponentially towards conduction band edge such that this suggests interface states in both SBDs are donor type. Also, it is seen that dispersing $HAuCl_4$ in the block polymer caused the interface states localize further from conduction band into the band gap.

4 Conclusions

For the purpose of investigating usefulness of PPG-b-PS in SBDs, MPS1 and MPS2 structures were fabricated and their *I-V* measurements were held at room temperature for electrical characteristics analysis. Experimental results showed that both SBDs perform good rectifying behavior with a RR value (~10^4) thanks to high R_{sh} and low R_s values. Moderate n values were obtained for the SBDs, however larger values of n (than unity) indicated TE may not be the dominant CCM. It was found that several CCMs are dominant in the whole forward bias region utilizing ln*I*-ln*V* plots of the SBDs. When compared to SBDs with commercial interfacial polymer layer in the literature, use of PPG-b-PS block copolymer as interfacial layer leads to improvements in the electronic parameters of the structures.

Acknowledgements

This work is supported financially by Turkish Scientific Research Council (Grants Numbers: 110T884, 211T016), Düzce University Scientific Research Project (Project No's: 2011.05.03.068, 2011.05.HD.026, 2012.05.02.110, 2012.05.HD.052, 2013.05.02.195), and Bülent Ecevit University Research Fund (Grant Number: 2012-10-03-03).

References

1 Gullu O & Turun A, *Microelectron Eng*, 87 (2010) 2482.
2 Sahingoz R, Kanbur H, Voigt M & Soykan C, *Synth Met*, 158 (2008) 727.
3 Serrano W, Melendez A, Ramos I & Pinto N J, *Polymer*, 55 (2014) 5727.
4 Chen J Y, Chen H C, Lin J N & Kuo *C, Mater Chem Phys*, 107 (2008) 480.
5 Kim H R, Kim B S & Kim I S, *Mater Chem Phys*, 135 (2012) 1024.
6 Dasdemir M, Topalbekiroglu M & Demir A, *J Appl Polym Sci*,127 (2013) 1901.
7 Aytimur A, Kocyigit S, UsluI, Durmusoglu S & Akdemir A, *Curr Appl Phys*, 13 (2013) 581.
8 Hayat K, Shah S S, Yousaf M, Iqbal M J, Ali M, Ali S, Ajmal M & Iqbal Y, *Mater Sci Semicon Proc*,41 (2016) 364.
9 Aydogan S, Saglam M & Turut A, *Polymer*, 46 (2005) 10982.
10 Mustafa M K, Abdullah M M, Noori Z T M & Mustefa A, *Indian J Pure Appl Phys*, 53 (2015) 617.
11 Gokcen M, Tunc T, Altindal S & UsluI, *Mater Sci Eng*, 177 (2012) 416.
12 Gokcen M, Tunc T, Altindal S & UsluI, *Curr Appl Phys*, 12 (2012) 525.
13 Gunduz B, Yahia I S & Yakuphanoglu F, *Microelectron Eng*, 98 (2012) 41.
14 Sathish S & Shekar B C, *Indian J Pure Appl Phys*, 52 (2015) 64.
15 Sonmezoglu S, Senkul S, Tas R, Cankaya G & Can M, *Solid State Sci*, 12 (2010) 706.
16 Henderson I M, Adams P G, Montano G A & Paxton W F, *J Polym Sci Polym Phys*, 52 (2014) 507.
17 Jeong B, Bae Y H , Lee D S & Kim S W, *Nature*, 388 (1997) 860.

18 Del C Pizarro G, Marambio O G, Jeria-Orell M, Gonzaez-Henriquez C M, Sarabia Vallejos M & Geckeler K E, *Express Polym Lett*, 9 (2015) 525.

19 Goosen M F & Sefton M V, *J Biomed Mater Res*, 13 (1979) 347.

20 Forster S & Plantenberg T, *Angew Chem Int Edit*, 41 (2002) 688.

21 Kumar N, Majeti N V, Ravikumar A & Domb A J, *Adv Drug Del Rev*, 53 (2001) 23.

22 Cheng S K,Wang C C & Chen C Y, *Mater Chem Phys*, 78 (2003) 581.

23 Alli A, Hazer B, Menceloglu Y Z & Suzer S, *Eur Polym*, 42 (2006) 740.

24 Hansen K K, Nielsen C J & Hvilsted S, *J Appl Polym Sci*, 95 (2005) 981.

25 Durmaz H, Dag A, Hizal A, Hizal G & Tunca U, *J Polym Sci Polym Chem*, 46 (2008) 7091.

26 Arslan H, Hazer B & Kowalczuk M, *J Appl Polym Sci*, 85 (2002) 965.

27 Macit H & Hazer B, *J Appl Polym Sci*, 93 (2004) 219.

28 Degirmenci M, Cianga I & Yagci Y, *Macromol Chem Phys*, 203 (2002) 1279.

29 Hazer B, *Synthesis and characterization of block copolymers*, in Handbook of polymer science and technology, (New York: Marcel Dekker), 1989.

30 Walz R, Bomer B & Heitz W, *Macromol Chem Phys*, 178 (1977) 2527.

31 Hazer B, *Macrointermediates for block and graft copolymers*, in Handbook of engineering polymeric materials, (New York: Marcel Dekker), 1997.

32 Dicke H R & Heitz W, *Macromol Rapid Commun*, 2 (1981) 83.

33 Anand P S, Stahl H G, Heitz W, Weber G & Bottenbruch L, *Macromol Chem Phys*, 183 (1982) 1685.

34 Laverty J J & Gardlund Z G, *J Polym Sci Polym Chem*, 15 (1977) 2001.

35 Haneda Y, Terada H, Yoshida M, Ueda A & Nagai S, *J Polym Sci Polym Chem*, 32 (1994) 2641.

36 Gokcen M, Yildirim M, Demir A, Alli A, Alli S & Hazer B, *Compos Part B Eng*, 57 (2014) 8.

37 Gokcen M & Alli A, *Philos Mag*, 94 (2014) 925.

38 Frukawa J, Takamori S & Yamashita S, *Macromol Mater Eng*, 1 (1967) 92.

39 Bilkan C, Zeyrek S, San S E & Altindal S, *Mat Sci Semicon Proc*, 32 (2015) 137.

40 Norde H, *J Appl Phys*, 50 (1979) 5052.

41 Cheung S K & Cheung N W, *Appl Phys Lett*, 49 (1986) 85.

42 Nicollian E H & Brews J R, *MOS physics and technology*, (Wiley: New York), 1982.

43 GokcenM & Yildirim M, *Chin Phys B*, 21 (2012) 128502.

44 Durmuş P &Yildirim M, *Mater Sci Semicon Proc*, 27 (2014) 145.

45 Kaya A, Sevgili O, Altindal S & Ozturk M K, *Indian J Pure Appl Phys*, 53 (2015) 56.

46 Khan S M, Sayyad M H & Karimov K S, *Ionics*, 17 (2011) 307.

47 Card H C & Rhoderick E H, *J Phys D: Appl Phys*, 4 (1971) 1589.